Reaction channels for the catalytic oxidation of CO on Pt(111)

A. Eichler and J. Hafner*
Institut für Theoretische Physik and Center for Computational Materials Science, Technische Universität Wien, Wiedner Hauptstrasse 8-10, A-1040 Wien, Austria
(Received 3 August 1998)

The catalytic oxidation of CO on O-precovered Pt(111) surfaces has been modeled via *ab initio* local-density-functional calculations. It is shown that at coverages of $\Theta_O \sim 0.5$ the coadsorption of CO stabilizes the chemisorbed molecular precursor of O_2 over the dissociated atomic oxygen. The barrier for the reaction between the coadsorbed molecules is lowest if first the molecular O_2 bond is broken. However, at this high coverage the barrier for the O_2+CO reaction is higher than for O_2 desorption. Therefore oxidation will be preceded by a partial desorption of O_2. At reduced coverage, the barrier for the oxidation reaction is strongly reduced. At the transition state the nascent O atoms are only bridge or top bonded and therefore quite reactive. After desorption of CO_2, the adsorbed atomic O can react with a second CO molecule via a transition state similar to that for the molecular reaction. [S0163-1829(99)07807-8]

I. INTRODUCTION

Platinum is together with Rh, Pd, and Ir among the most widely used industrial catalysts. Especially important is the use of Pt in catalytic converters for the post-combustion oxidation of CO and reduction of NO_x. This technological importance led to an enormous effort directed towards the understanding of the rather simple catalytic oxidation of CO on Pt(111).[1–15] Until recently a quantum-mechanical modeling of the reaction has been impossible, so that the only information available came from experiments and classical kinetic computer simulations.[4,6]

The aim of this study is to shed light onto the catalytic oxidation of CO to CO_2 on an oxygen precovered Pt(111) surface via *ab initio* total-energy calculations. We investigate various reaction channels for this reaction and identify the corresponding transition states (TS's).

The paper is organized as follows: we start with an overview of the experimental situation in Sec. II, followed by a brief description of the theory our calculations are based on (Sec. III). In Sec. IV we give a comparison of various (co)adsorption structures representing possible start, intermediate, and final configurations for the oxidation reactions. Concerning the reaction itself, we distinguish between a bimolecular reaction A, $CO(g)+O_2(g)\rightarrow CO(a)+O_2(a)\rightarrow O(a)+CO_2(g)$, involving the coadsorption of molecular oxygen and CO and their direct reaction producing CO_2 and adsorbed oxygen, and reaction B of CO with atomic O on the surface, $CO(g)+\frac{1}{2}O_2(g)\rightarrow CO(a)+O(a)\rightarrow CO_2(g)$. The bimolecular reaction A is discussed in Sec. V, the reaction between the already dissociated O atoms and CO in Sec. VI.

II. EXPERIMENTAL SITUATION

Below temperatures of $T\approx 100$ K, O_2 adsorbs molecularly on the Pt(111) surface in two modifications: a paramagnetic superoxo state (O_2^-), which is formed at the bridge site in a flat *t-b-t* geometry,[16] and a nonmagnetic peroxo state (O_2^{2-}) located at the hollow site in a slightly canted *t*-fcc-*b* configuration[17,18] (compare Fig. 1). The saturation coverage for this structure is about $\Theta_{O_2}=0.45$ monolayers (ML).[19,20] Raising the temperature above 160 K results in the desorption of about half of the molecules. The remaining O_2 molecules dissociate into the fcc hollows forming a $p(2\times 2)$ structure at an atomic coverage of $\Theta_O=0.25$.

Coadsorption of CO at the O_2 precovered surface below 160 K leads to on-top adsorption up to a coverage of Θ_{CO}

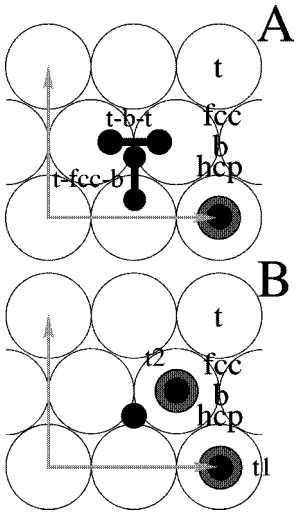

FIG. 1. Sketch of the surface cell used for our calculations. The open circles denote the positions of the surface Pt atoms, the letters on the right hand side the high-symmetry positions (*t*, top; fcc, fcc hollow; *b*, bridge; hcp, hcp hollow). In the upper panel (A) the positions of the CO molecule (combined grey-black disks in an on-top position) together with the two possible O_2 precursors (black dumb bells in *t-b-t* and *t*-fcc-*b* configurations) are drawn, as they are used for reaction A (cf. text). The surface coverage is $\Theta_{O_2}=0.25$ (corresponding to $\Theta_O=0.5$) and $\Theta_{CO}=0.25$. The lower panel shows the starting positions for reaction B with the O atom (small black disk) in the fcc hollow and the CO molecule in the $t1$ and $t2$ positions, respectively (cf. text). The coverage is $\Theta_O=0.25$ and $\Theta_{CO}=0.25$.

$=0.25$–0.30 ML.[9,11] Upon heating to about 125–160 K part of the O_2 desorbs and oxidation of CO to CO_2 starts. Several peaks of CO_2 desorption have been observed: The first (α) peak has been observed at 125–160 K,[3,7,10,11] i.e., at the temperature where the desorption of O_2 starts. This peak has only been observed when molecular oxygen is present on the surface and has therefore been attributed to the reaction of nascent or hot O atoms provided by O_2 dissociation with the CO molecule. Another set of desorption peaks (β_3,β_2,β_1) is located in the temperature range where O_2 is already dissociated ($T=200$–225, 250–260, and 260–330 K, respectively[3,7,10,11]). For the completely ordered $p(2\times2)$ structure only the β_1-desorption peak has been observed; the β_2 and β_3 peaks have been assigned to disordered CO-O overlayers.[11] The oxidation resulting in the β_1 peak is believed to occur via a Langmuir-Hinshelwood mechanism, which means that the reaction takes place between the chemisorbed reagents. From the analysis of the angular and velocity distributions of desorbing CO a very similar TS to that for the α desorption has been proposed for this channel.[10] Similar reactions have been induced also by collision with Xe atoms[12] and photons.[5,9,13] Finally the resulting CO_2 molecule is weakly bound to the surface [$E^{\mathrm{ad}}_{CO_2}$ ~ 2.5 kcal/mol (Ref. 3)] before it desorbs.

III. THEORY

Our calculations have been performed using a spin-polarized version of the Vienna *ab initio* simulation program (VASP).[21,22] VASP performs an iterative solution of the generalized Kohn-Sham equations of local-spin-density (LSD) theory via an unconstrained minimization of the norm of the residual vector to each eigenstate and optimized routines for charge- and spin-density mixing. The calculations are performed in a plane-wave basis, using fully nonlocal Vanderbilt-type ultrasoft pseudopotentials to describe the electron-ion interaction.[23] Exchange and correlation are described by the functional proposed by Perdew and Zunger,[24] adding nonlocal corrections in the form of the generalized-gradient approximation (GGA) of Perdew *et al.*[25] Although this functional provides a substantial improvement compared to the LSD approximation (LSDA), there are still substantial errors, especially for the binding energies of the free molecules, whereas the bond lengths and frequencies are predicted rather accurately (see Table I). For the CO_2 molecule the overbinding is still rather pronounced, leading to an overestimation of the heat of reaction for the oxidation reaction $CO+\frac{1}{2}O_2\rightarrow CO_2$ in the gas phase ($\Delta H^g_{\mathrm{calc}}=3.41$ eV, $\Delta H^g_{\mathrm{expt}}=2.94$ eV).

The Pt(111) substrate is modeled by a four-layer slab with a rectangular $\sqrt{3}\times2$ unit cell [equivalent to a $c(4\times2)$ structure; compare Fig. 1] containing four substrate atoms, separated by a 14-Å-thick vacuum layer. All molecules are adsorbed on both sides of the slab. The effects of an increased thickness of the slab (up to eight layers) and of substrate relaxation have been tested and found to be small. We have neglected substrate relaxation effects since in our preceding calculations for the adsorption of O_2 on Pt(111) (Refs. 17 and 26) and CO on Rh(100) (Ref. 27) and Pd(100) (Ref. 28) we found only a minor influence of the substrate relaxation on the energetics and geometry of the adsorbate. To test the variation of the reaction barriers as a function of coverage, a few calculations with a doubled surface cell ($\sqrt{3}\times4$) have been performed.

TABLE I. Binding energies, bond lengths, and stretching frequencies for O_2, CO, and CO_2 molecules.

	E_b(eV)	d(Å)	ω (cm^{-1})
	O_2		
GGA	6.44	1.24	1552
Expt.	5.2	1.21	1580
	CO		
GGA	11.58	1.15	2114
Expt.	11.2	1.13	2170
	CO_2		
GGA	18.14	1.17	1316
Expt.	16.73	1.16	1333

Brillouin-zone integrations have been performed on a grid of $3\times4\times1$ $\vec{k}$ points, using a Methfessel-Paxton smearing[29] of $\sigma=0.2$ eV. All calculations have been performed at the equilibrium lattice constant of $a=3.99$ Å (experiment: $a=3.92$ Å). Convergence tests for the adsorption of O_2 on Pt(111) (Ref. 17) have shown that this setup is converged with respect to slab thickness, vacuum spacing, and $\vec{k}$-point sampling.

To determine the activation energies of the reactions, the TS's have been determined using the nudged elastic band (NEB) method.[30] In this method the total energies of a series of intermediate states distributed along the reaction path connecting the starting and final states are simultaneously minimized, restricting the atomic motions to the hyperplane perpendicular to the reaction path. In our case the starting state is given by the adsorbed CO molecule and a coadsorbed O_2 molecule or O atom; the final state is the free CO_2 molecule (plus eventually an O atom adsorbed on the surface). The simplest way to construct a starting approximation to a possible reaction path is a linear interpolation between the starting and final states, but the interaction with the substrate may suggest a different intermediate geometry.

IV. MOLECULAR ADSORPTION AND COADSORPTION

In Table II the adsorption energies for various combinations of the adsorbates during the reaction are compiled. The energy zero for reaction A is set to the sum of the energies of the clean surface and the free O_2 and CO molecules, representing the starting point of the reaction. The energy zero for reaction B is set to the energy of half an oxygen molecule less. In other words reaction A describes the bimolecular reaction at $\Theta_O=0.5$, while reaction B takes place at $\Theta_O=0.25$ between the adsorbed atoms and the CO molecules.

A. (Co)adsorption structures during the reaction of molecular oxygen and carbon monoxide

In reaction A first O_2 is adsorbed at the surface ($\Theta_{O_2}=0.25$) in one of the two molecular precursors, the paramag-

TABLE II. Adsorption energies and coadsorption energies for various combinations of adsorbates (characterized by the left part of the table: the letters denote the adsorption position; *g* stands for gas phase) in eV/surface cell; the first line in part A, A′, and B defines the energy zero (molecules in the gas phase). The experimental values have been taken from Refs. 3,14,19, and 35.

	O	O_2	CO	CO_2	E^{calc} [eV]	E^{expt} [eV]
	–	*g*	*g*	–	≡0.0	–
	–	*t*-*b*-*t*	*g*	–	0.72	0.4-0.5
	–	*t*-fcc-*b*	*g*	–	0.68	0.4-0.5
	2×fcc	–	*g*	–	1.65	1.4
A [a]	–	*g*	*t*	–	1.58	1.66
	–	*t*-*b*-*t*	*t*	–	2.36	?
	–	*t*-fcc-*b*	*t*	–	2.30	?
	2×fcc	–	*t*	–	1.95	?
	fcc	–	–	*g*	4.39	3.79
	–	*g*	*g*	–	≡0.0	–
A′ [b]	–	*t*-fcc-*b*	*t*	–	2.58	?
	2×fcc	–	*t*	–	3.14	?
	–	1/2*g*	*g*	–	≡0.0	–
	fcc	–	*g*	–	0.98	0.85
	hcp	–	*g*	–	0.61	?
B [c]	fcc	–	*t*1	–	2.56	?
	hcp	–	*t*1	–	2.18	?
	–	–	–	*t*	0.06	~0.1
	–	–	–	*g*	3.41	2.94

[a] $\Theta_{O_2}=\Theta_{CO}=1/4$.
[b] $\Theta_{O_2}=\Theta_{CO}=1/8$.
[c] $\Theta_O=\Theta_{CO}=1/4$.

netic superoxo *t*-*b*-*t* state or the nonmagnetic peroxo *t*-fcc-*b* state[17,18] (compare Fig. 1). [For a more detailed characterization of the precursor states see our previous work[17] and recent scanning tunnel microscope (STM) studies[18].] These precursors are metastable at low temperature with respect to dissociation into two oxygen atoms adsorbed in the fcc hollows in a $p(2\times2)$ geometry. However, the barrier for dissociation at this coverage is even ~0.15 eV higher than the desorption energy,[17,26] in agreement with the experimentally determined atomic coverage of only $\Theta_O=0.25$ in the $p(2\times2)$ geometry, indicating that half of the oxygen desorbs prior to dissociation.

CO adsorbs in molecular form on Pt(111), bonding through the C atom to the on-top site in an upright geometry. At a coverage of $\Theta_{CO}=0.25$ the adsorption energy is 1.58 eV—as for oxygen adsorption we find good agreement with the experimental estimates (see Table II). Coadsorption of CO and molecular oxygen leads to a small energy gain relative to the sum of the adsorption energies of the two species (0.06 eV and 0.04 eV for O_2 in the *t*-*b*-*t* and *t*-fcc-*b* precursors, respectively). Coadsorption of CO and atomic oxygen, on the other hand, results in an energy loss of −1.28 eV so that after coadsorption the molecular state of oxygen is stabilized relative to the dissociated state: the adsorption energy is 2.36 eV (2.30 eV) for O_2 in the *t*-*b*-*t* and *t*-fcc-*b* precursors and CO on top, and 1.95 eV for two O in fcc hollows and CO on top (see Table II).

We also note that there is no barrier for CO adsorption on the oxygen precovered surface. In the last step the coadsorbed CO and O_2 react to form CO_2 (gas phase or weakly physisorbed) and adsorbed atomic O. This reaction is analyzed in Sec. V.

The energy of the final state is the sum of the adsorption energy of O at $\Theta_O=0.25$ ($E^{ad}=0.98$ eV) and the difference in the binding energies of the reactants in the gas phase, $\Delta H^g=3.41$ eV, which is $\Delta H^A=4.39$ eV. The rate-limiting step will be the barrier for the reaction between coadsorbed CO and O_2. The coadsorption energies are strongly coverage-dependent. At the coverage of $\theta_{O_2}=\theta_{CO}=1/8$ the stability of the molecular and atomic adsorbed oxygen is reversed (see part A′ in Table II). This emphasizes the important role of lateral adsorbate-adsorbate interactions.

B. (Co)adsorption structures during the reaction of atomic oxygen and carbon monoxide

Reaction B starts with the dissociation of $\frac{1}{2}O_2$. This process results in an O-covered surface at $\Theta_O=0.25$, the same structure that was the final stage of reaction A. The adsorption energy is 0.98 eV. A determination of the dissociation barrier at the given coverage would require calculations based on a doubled supercell (the present cell contains only a single O atom). Considering the pronounced coverage dependence of the O binding energy (see Table II) and from a comparison with experiment it can be assumed that the barrier decreases probably below that for desorption of the chemisorbed molecule. For the coadsorption of 0.25 ML CO in on-top sites there are two possibilities (compare Fig. 1): one situation with CO and O being at maximal distance ($t1$) and a second with the CO sitting on a substrate atom near the O-occupied hollow ($t2$). Placing the CO molecule at $t2$ a repulsive interaction between CO and O dominates, which leads to a decrease of the adsorption energy and a shift of the O out of its hollow position towards the neighboring bridge position, which means that a situation with an O atom adsorbed in a hollow and a CO molecule occupying a neighboring substrate atom is not a stable position.

Experimentally it was found that the adsorption of CO on O-precovered surfaces with the O atoms adsorbed in the threefold hollows in a (2×2) geometry leads to low-energy electron diffraction (LEED) patterns and high-resolution electron-energy-loss spectroscopy (HREELS) signals compatible with on-top adsorbed CO in a (2×2) symmetry.[31]

The adsorption of CO on $t1$ and of atomic O in the hollow on the other hand is a completely independent process. The sum of the individual adsorption energies equals exactly the coadsorption energy. Adsorption of CO on the O-precovered surface is—similar to reaction A—again a nonactivated process. The final reaction produces again a slightly physisorbed CO_2 molecule that will desorb from the afterwards clean surface. The total heat of reaction for reaction B is equivalent to the gas-phase reaction energy ($\Delta H^g=\Delta H^B=3.41$ eV).

V. BIMOLECULAR REACTION OF CO WITH COADSORBED O_2

To determine the activation energies in both reaction channels, the TS's have been determined using the nudged

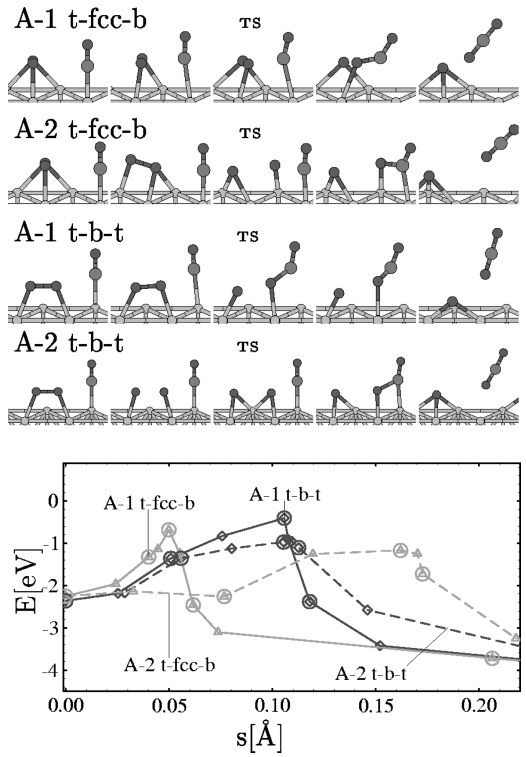

FIG. 2. Reaction paths and energetic profile for reaction A: The upper panel shows sketches of the optimized states along each reaction path. In the lower panel the energy of these reaction pathways is plotted as a function of the linear distance between the states (all pathways are cut at a reaction coordinate of $s = 0.22$ Å, for the final state, CO_2 in the gas phase; the final energies of all pathways are equal). Positions that are shown in the upper panel are marked with circles. The energy zero is set to the energy of the free molecules plus the clean slab (compare Fig. 5.)

elastic band method.[30] Since in this method a starting reaction path is optimized, it may happen that the obtained transition state is not necessarily the lowest.

To cope with such a situation we have considered two alternative scenarios: In the first (A-1), we assumed a direct reaction of O_2 with the CO molecule approaching the molecularly absorbed O_2. The initial state is given by the coadsorbed molecules, the final state by an O atom adsorbed in a threefold hollow and CO_2 desorbing from the surface. The starting path for the NEB method is a linear interpolation between the coordinates of the initial and final states. In the second scenario (A-2) we assume that the O_2 dissociates before reacting with CO. In this case we took an additional intermediate configuration with the O_2 molecule dissociated into two O atoms in hollow positions. The NEB starting path is the concatenation of a linear interpolation between the start and the intermediate configuration and the intermediate and the final one.

Since we wanted to restrict the computational effort and we are mainly interested in the height of the energy barrier, we took only eight (relaxing) states (between the two fixed boundary configurations) along each reaction path with smaller distances in the region of the TS's.

A. High coverage ($\Theta_{O_2} = \Theta_{CO} = 1/4$)

The results obtained for a high coverage of both O_2 and CO are shown in Fig. 2, where also the energy as a function of the linear distance between the states is plotted for each path. In Table III the barrier heights with respect to the preceding minimum as well as the geometries at the TS's are compiled. Starting from the *t*-fcc-*b* peroxo precursor, the barrier is 1.62 eV along the reaction channel A-1 and 1.18 along channel A-2. Starting from the *t-b-t* superoxo precursor, the barrier heights are 1.93 eV (A-1) and 1.41 eV (A-2), respectively. Increasing the slab thickness and/or relaxation of the substrate changes the barrier heights by at most 0.15 eV.

TABLE III. Energy barrier E_{barr} with respect to the preceding potential well [for reaction A coadsorption of the molecular O_2 precursor with CO; for the Langmuir-Hinshelwood (LH) reaction B all barrier heights are given with respect to O in the fcc hollow, CO on top; for the Eley-Rideal (ER) reaction the energy zero is given by an adsorbed O atom and a free CO molecule] in eV at the transition states and geometric values: height of the reacting O (z_O), distances of the dissociated O atoms (d_O), height of the C above the surface (z_C), and bond lengths of the just formed CO_2 molecule (d_1,d_2) in Å and bond angle α.

			E_{barr}	z_O	d_O	z_C	d_1	d_2	α
A[a]	1	*t*-fcc-*b*	1.62	1.61	1.84	2.29	1.89	1.17	113°
	2		1.18	1.47	2.19	1.92	2.15	1.16	107°
	1	*t-b-t*	1.93	1.75	2.02	2.51	1.66	1.17	125°
	2		1.41	1.44	2.51	2.04	2.52	1.17	116°
A′[b]	2	*t*-fcc-*b*	0.46	1.47	2.19	1.92	2.15	1.16	107°
B[c]	LH	fcc	0.79	1.43	–	1.71	3.03	1.16	102°
			0.75	1.53	–	1.88	2.02	1.16	112°
	LH	hcp	0.68	1.44	–	1.59	3.48	1.17	94°
			0.73	1.51	–	1.87	2.15	1.16	107°
	ER	fcc	0.75	1.63	–	2.78	1.73	1.16	127°

[a] $\Theta_{O_2} = \Theta_{CO} = 1/4$.
[b] $\Theta_{O_2} = \Theta_{CO} = 1/8$.
[c] $\Theta_O = \Theta_{CO} = 1/4$.

In the transition state the just formed CO_2 molecule is bent by approximately 110°–130°, with the oxygen atom from the CO molecule pointing upwards, similar to the TS's proposed in Refs. 4 and 8. The barrier is always lower if dissociation of O_2 occurs first (reaction path A-2). However, at the TS's the dissociated O atoms do not occupy the stable positions in the threefold hollow, but are only bridge and top bonded (channel A-2 *t*-fcc-*b*), respectively, both bridge bonded (channel A-2 *t-b-t*) and therefore more reactive. The *t*-fcc-*b* peroxo precursor as a starting point leads to a lower barrier for the direct reaction (A-1) as well as for the reaction with previous dissociation of O_2 (A-2). This has mainly two reasons: first the O-O bond in the *t-b-t* superoxo precursor is stronger than that for the peroxo state[17] and hence the energy necessary for the dissociation is higher. This is also reflected by the smaller C-O bond length d_1 for the A-1 reactions, since the CO has to be nearer to the oxygen molecule in the *t-b-t* state than for the *t*-fcc-*b* state, so that the C-O attraction is strong enough to dominate over the O-O bond and break the molecule up. The second reason is that the potential energy surface (PES) surrounding the *t*-fcc-*b* precursor is less corrugated which makes it easier for the molecule to move into a position which favors the reaction. For both

reaction channels (A-1 t-fcc-b and A-2 t-fcc-b) the O_2 molecule initiates the reaction with a rotation into an equivalent position by 30° so that the bridge-bonded O atom is pointing towards the CO molecule.

When the molecular O_2 bond is already broken before the reaction takes place (scenario A-2), the attraction between CO and O is effective already for larger distances d_1, resulting in a lower energy barrier. Also for the A-2 pathways the reaction starting from the t-fcc-b O_2 precursor has the lower-energy barrier, although the TS's look rather similar. One reason for that is the higher symmetry of the t-b-t precursor, which suppresses the asymmetric bond breaking of the O_2 leading to a bridge-bonded and a predominantely linear bonded O atom as in the more favorable TS's in the t-fcc-b A-2 reaction (compare Fig. 2).

Analyzing the remaining geometric parameters, it becomes obvious that the energy barrier decreases the closer the TS is located to the surface (i.e., low z_O, z_C). So the lowest barrier is found in the reaction channel A-2 t-fcc-b passing through the dissociation of the adsorbed O_2 molecule, the transfer of one of the dissociated O atoms to a position (somewhere between bridge and on top) close to the adsorbed CO atom and reaction to a bent CO_2 molecule. This reaction allows a closer approach of both the dissociated O atom and of the C atom in the CO molecule to the surface.

To summarize, the limiting step for reaction A is the dissociation of the O_2 molecule on the surface. The CO molecules at the TS's of the A-2 reactions remain essentially in their initial geometry. This reaction provides two nascent O atoms, one of which reacts with a coadsorbed CO molecule forming CO_2.

B. Low coverage ($\Theta_{O_2}=\Theta_{CO}=1/8$)

A serious problem of this model for the reaction is the very high coverage. The repulsive interaction with the periodic images of the CO restrict the mobility of the O_2 molecules and raise therefore the barrier height. Furthermore, it has been experimentally observed for this coverage regime (compare Sec. II) that the reaction starts as soon as O_2 starts to desorb, i.e., as soon as locally the coverage is decreased. To get a feeling for the coverage dependence of the reaction barrier we recalculated the energy barrier in a laterally doubled cell ($\sqrt{3}\times 4$), the second half of the cell remaining empty. To simplify the calculations, we postulate the same TS geometry for both coverages. In this case ($\Theta_{CO}=1/8$, $\Theta_{O_2}=1/8$) the energy of the starting point of the reaction (O_2 in t-fcc-b, CO in $t1$) decreases by 0.28 eV and the barrier is dramatically reduced to 0.46 eV. We have verified that the forces acting on the atoms in the TS geometry are very small also for the large cell. Therefore we can assume that we are not too far from the exact transition state.

Our calculations do not exclude the possibility of the simultaneous reaction of the second nascent O atom with a further CO molecule according to the reaction $2CO+O_2 \rightarrow 2CO_2$, as has been proposed by Matsushima,[3] since this reaction has the same TS's related to the prior dissociation of O_2. However, to model a reaction like this a supercell with a doubled size is required, since in our geometry we have only one CO molecule per supercell.

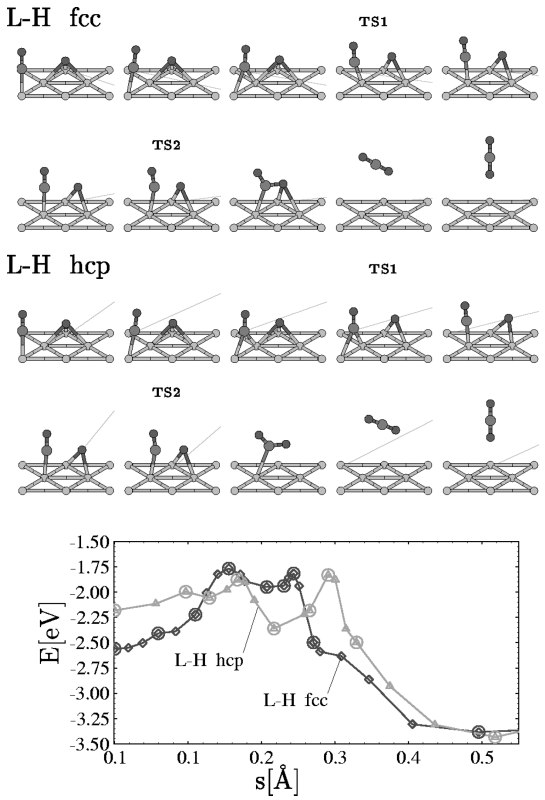

FIG. 3. Reaction paths and energetic profile for the Langmuir-Hinshelwood reaction B: The upper panel shows sketches of the optimized states along each reaction path. In the lower panel the energy of these reaction pathways is plotted as a function of the linear distance between the states. Positions that are shown in the upper panel are marked with circles. The energy zero is set to the energy of the free molecules plus the clean slab (compare Fig. 5)

VI. REACTION OF CO WITH DISSOCIATED O

This reaction can occur with previously dissociated oxygen, but it also can be seen as a follow up reaction of the previously described bimolecular reaction. The desorbing CO_2 molecule leaves behind an O atom adsorbed in a threefold hollow. Adsorption of another CO leads to an O-CO coadsorption structure with $\Theta_O=\Theta_{CO}=0.25$. A possible starting reaction path for the NEB method represents again a linear interpolation between the starting configuration (compare Figs. 1 and 3) and a CO_2 molecule desorbing from the surface above a prior O-occupied (fcc) hollow position. This implies that the CO molecule has to approach via the hollow position at a height suitable for a reaction with the O atom. The consequence is a kind of pickup reaction. However, this leads to a very high reaction barrier of 2.33 eV. The reason that an approach across the hollow is energetically extremely unfavorable is that two of the three substrate atoms constituting the hollow are already passivated by the neighboring O atom, so that the CO molecule has essentially to desorb before reacting with the O atom. We will come back to this reaction channel at the end of this section.

An alternative scenario, obtained using a slightly modified starting path for the NEB method, is shown as path fcc in Fig. 3: the CO molecule approaches the O atom not directly along the path across the unoccupied hollow (see Fig. 1), but moves first from $t1$ to $t2$ via the intermediate bridge posi-

tion. When moving from $t1$ to $t2$, the CO molecule pushes the O atom out of the hollow position into a bridge geometry. This first O-substrate bond breaking is the reason for the first barrier ($E_{\mathrm{barr}}=0.79$ eV, fourth image in Fig. 3) leading into a shallow local minimum with a CO molecule adsorbed on site $t2$ and the O atom in the neighboring bridge position. The reaction then takes place by pushing the CO molecule towards the now bridge-bonded oxygen atom. The attraction between the C atom and the adsorbed O atom breaks then a second O-substrate bond, so that immediately after the transition state ($E_{\mathrm{barr}}=0.75$ eV) a bent CO_2 molecule is weakly bound through the C and one O atom to two substrate atoms which leaves the surface nearly parallel to it. This ''flat'' CO_2 desorption geometry can be observed also for the later discussed hcp path and is a hint at a weak physisorption in this geometry. The tilting up of the molecule at the end of the path is related to the chosen end configuration.

We have also investigated the corresponding reaction path starting with O adsorbed in the hcp hollows. Although the initial position is higher in energy by 0.36 eV, the two barriers (shifting CO from $t1$ to $t2$ and the reaction itself) are of about the same height (with respect to O in the fcc hollow, CO in $t1$). For this reaction channel the local minimum for CO in $t2$ and O in the bridge is much more pronounced with the O atom being slightly nearer to the fcc than to the hcp hollow (see the fifth image of path hcp in Fig. 3). The geometry is already very similar to the starting configuration of the fcc path (O in the fcc hollow, CO in $t1$) and therefore also the energy became comparable (lower than in the starting configuration: O in the fcc hollow, CO in $t1$). In contrast to the fcc path the reaction does not continue with another CO shift, pushing the O atom onto a bridge site, but the O atom crosses again the bridge back towards the hcp hollow and the reaction takes place around the hcp hollow. This shows that the previousely discussed B-fcc reaction is not the only pathway passing through the lowest TS. Alternatively to the CO movement also the O atom can initiate the reaction by leaving the fcc hollow and approaching the CO molecule (images 5-10 of path hcp in Fig. 3).

It is remarkable that the TS's for reactions fcc and hcp (seventh image in Fig. 3, Table III) are geometrically very similar to those for reaction A (A-2 t-fcc-b); cf. Table III. This similarity between the TS's for the bimolecular reaction and the reaction with adsorbed O atoms has already been predicted by Allers *et al.*[10] on the basis of angular and velocity distributions of the CO_2 product molecules in the α and β_1 desorption peaks (compare Sec. II).

Again a small CO_2 bond angle in combination with a long C-O (a) distance and a low z_{C} favors the reaction.

A similar TS for the reaction B has very recently been described for the same system by Alavi *et al.*[33] They found a C-O(a) distance of 2.1 Å and a barrier height of 1.05 eV (GGA). The difference in barrier heights can be attributed to the different setups in the calculations (only three atomic layers in the slab modeling the substrate, different surface cell geometry $[p(2\times2)]$, Brillouin-zone integrations with $(2\times2\times1)\vec{k}$-point-grid only, norm-conserving pseudopotentials).

The calculated barrier height is in good agreement with experimental estimates for reaction B from Refs. 1 and 2 at about the same coverage ($E_{\mathrm{barr}}^{\mathrm{expt}}=0.51$ eV and 0.71 eV, respectively). Also a very recent scanning tunneling microscopy study[34] estimated a barrier height of about 0.49 eV.

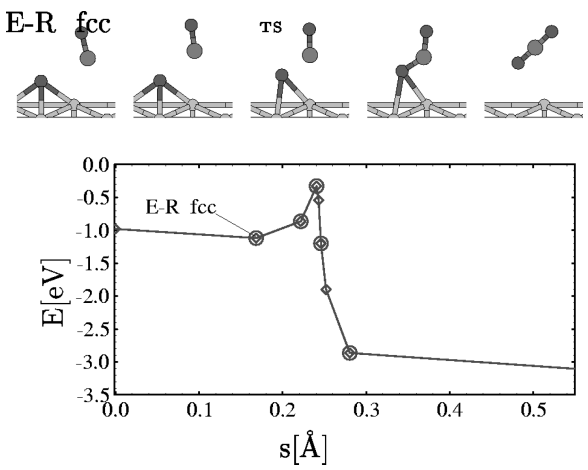

FIG. 4. Reaction paths and energetic profile for an Eley-Rideal reaction of gaseous CO with adsorbed atomic oxygen: The upper panel shows the variation of the geometry along the reaction path, the lower panel the energetic profile of the reaction. Positions that are shown in the upper panel are marked with circles. The energy zero is set to the energy of the free molecules plus the clean slab (compare Fig. 5 and text).

All reaction channels discussed so far assume a Langmuir-Hinshelwood mechanism, i.e., a reaction between the coadsorbed species. However, in the scenario discussed at the beginning of this section we have found that the starting path for the NEB method leads to a forced desorption of the CO molecule. This is a good example that—as mentioned above—a relaxation in the subspace perpendicular to some arbitrary reaction path does not necessarily explore all the configuration space available for the reaction. At the same time, this result allows us to explore the energetics of an Eley-Rideal reaction between an adsorbed O atom and an impinging CO molecule—in fact this is just the second part of the reaction path mentioned at the beginning of this section (after the CO molecule has been desorbed from the Pt substrate).

In this case the starting point is an adsorbed O atom and a free CO molecule close to the surface (see Fig. 4). Relative to this starting configuration the barrier height is only 0.75 eV, comparable to that for the Langmuir-Hinshelwood reaction. The transition state corresponds to a CO_2 molecule with one elongated ($d_1=1.16$ Å) and one short bond ($d_2=1.73$ Å) and a bond angle of 127°. This geometry is very similar to that for the Eley-Rideal reaction of CO with O adsorbed on Ru(0001) described by Stampfl and Scheffler.[32] We also note that the O-CO bond distance at TS's for the Eley-Rideal reaction is considerably shorter ($d_1=1.73$ Å) than that for the Langmuir-Hinshelwood reactions ($d_1=2.02$ Å; see Table III). This may be a further reason why the Langmuir-Hinshelwood reaction is favored in spite of similar barrier heights. Another important fact is the higher attempt frequencies for the Langmuir-Hinshelwood mechanism than in an Eley-Rideal reaction, which have not been determined within this study.

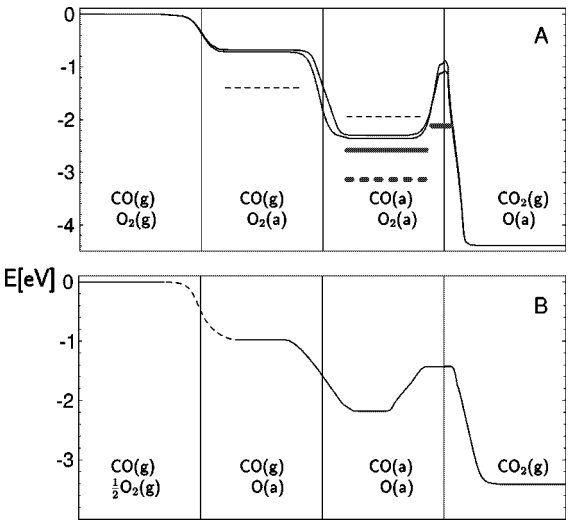

FIG. 5. Energy diagrams of reactions A (high coverage, thin lines; low coverage, thick lines) and B as a function of a one-dimensional reaction coordinate. The dashed lines for reaction A indicate the energies for the dissociated O_2 molecule, the bold gray lines the energies for the reaction at half coverage (reaction A′); cf. text.

VII. DISCUSSION AND CONCLUSIONS

We have presented detailed *ab initio* studies of different possible reaction channels for the catalytic oxidation of CO on Pt(111). The energetic profile of these reactions is compiled in Fig. 5.

Since we have collected quite a lot of information, we will now try to model the evolution of a coadsorption structure as it has been used in various thermal desorption spectroscopy (TDS) studies upon heating on the basis of our calculations. We start with the coadsorption structure at $\Theta_{CO}=0.25$ and $\Theta_O=0.5$. At this coverage coadsorption of CO stabilizes the peroxo- (superoxo-) like precursors over the dissociated atomic adsorbate. Desorption of O_2 costs about 0.75 eV, i.e., much less than the lowest barrier for the bimolecular reaction at this coverage ($E^{A}_{barr}=1.18$ eV). Hence the first step will be the desorption of some O_2 molecules [experimentally observed at 125–160 K (Refs. 3,7,11, and 12)]. This leads locally to a lower coverage and therefore to a lower barrier for the reaction A ($E^{A'}_{barr}\sim 0.46$ eV). Thus immediately after the O_2 desorption the bimolecular reaction takes place, consisting of the dissociation of the O_2 molecule and a subsequent reaction of a nascent (weakly bound) O atom with the CO molecule and the adsorption of the second one. This leads to the experimentally observed α peak in the TDS spectra at about 125–160 K.[3,7,11,12] At the TS's the dissociated O atoms are only bridge or top bonded and therefore quite reactive. It is also significant that the nonmagnetic peroxo precursor with an already more stretched O-O bond leads to a lower barrier.

At this stage of the reaction atomic oxygen is adsorbed at the surface: part of it as end product of reaction A, part from O_2 dissociation without subsequent reaction to CO_2. After further heating the atomic oxygen reacts with CO ($E^{B}_{barr}\sim 0.75$ eV) as reflected by the β_1 peak in the TDS spectra. The barrier height is in nice agreement with experimental predictions of $E^{expt}_{barr}=0.5$–0.7 eV.[1,2,34] Reaction between the CO molecule and the O atom takes place along a reaction path minimizing the number of broken adsorbate-substrate bonds: the CO molecule moves first from the energetically more favorable on-top position (i.e., the one minimizing the CO-O repulsion) to one close to the O atom, pushing it out of the hollow to a neighboring bridge position. At the TS state the CO atom remains close to the on-top position and reacts with the bridge-bonded O_2 molecule.

In this connection it may be worth mentioning that Kostov *et al.*[31] have detected during the O+CO reaction an additional loss feature at $\omega=1850$ cm^{-1} ascribed to bridge-adsorbed CO. This can be considered as a further confirmation for the transition mechanism proposed in our paper.

Note that the TS states for both types of reactions are nearly identical (in agreement with experimental predictions,[10]) the common principle being that the reaction barrier is minimized if only the minimum number of adsorbate-substrate bonds are broken.

Altogether we have developed a complete scenario for the catalytic oxidation of CO on Pt(111) based on *ab initio* calculations.

ACKNOWLEDGMENTS

This work has been supported by the Austrian Science Foundation under Project No. P11353-PHYS. Computer time on a Cray T3E has been supplied by the Hochleistungsrechenzentrum für Wissenschaft und Forschung in Jülich.

*Present address: Institut für Materialphysik and Center for Computational Materials Science, Universität Wien, A-1090 Wien, Austria.

[1] C. T. Campbell, G. Ertl, H. Kuipers, and J. Segner, J. Chem. Phys. **73**, 5862 (1980).
[2] J. L. Gland and E. B. Kollin, J. Chem. Phys. **78**, 963 (1983).
[3] T. Matsushima, Surf. Sci. **127**, 403 (1983).
[4] D. W. J. Kwong, N. de Leon, and G. L. Haller, Chem. Phys. Lett. **144**, 533 (1988).
[5] W. D. Mieher and W. Ho, J. Chem. Phys. **91**, 2755 (1989).
[6] H.-P. Kaukonen and R. M. Nieminen, J. Chem. Phys. **91**, 4380 (1989).
[7] C. T. Rettner and C. B. Mullins, J. Chem. Phys. **94**, 1626 (1991).
[8] G. W. Coulston and G. L. Haller, J. Chem. Phys. **95**, 6932 (1991).
[9] W. D. Mieher and W. Ho, J. Chem. Phys. **99**, 9279 (1993).
[10] K.-H. Allers, H. Pfnür, P. Feulner, and D. Menzel, J. Chem. Phys. **100**, 3985 (1994).
[11] J. Yoshinubo and M. Kawai, J. Chem. Phys. **103**, 3220 (1995).
[12] C. Åkerlund, I. Zoric, and B. Kasemo, J. Chem. Phys. **104**, 7359 (1996).
[13] C. E. Tripa, Ch. R. Arumaninayagam, and J. T. Yates, Jr., J. Chem. Phys. **105**, 1691 (1996).
[14] Y. Y. Yeo, L. Vattuone, and D. A. King, J. Chem. Phys. **106**, 392 (1997).
[15] R. J. Finlay, T.-H. Her, C. Wu, and E. Mazur, Chem. Phys. Lett. **274**, 499 (1997).
[16] For the characterization of adsorption sites we use *t*, *b*, fcc, and hcp for the on-top, bridge, fcc hollow, and hcp hollow sites,

respectively. To describe the location of a molecule lying parallel to the surface a triple of sites is used: the letter in the middle indicates the position of the center of mass of the molecule, whereas the atoms are pointing towards the sites denoted by the first and last abbreviations.

[17] A. Eichler and J. Hafner, Phys. Rev. Lett. **79**, 4481 (1997).

[18] B. C. Stipe, M. A. Rezaei, W. Ho, S. Gao, M. Persson, and B. I. Lundqvist, Phys. Rev. Lett. **78**, 4410 (1997); B. C. Stipe, M. A. Rezaei, and W. Ho, Science **279**, 1907 (1998).

[19] H. Steininger, S. Lehwald, and H. Ihbach, Surf. Sci. **17**, 342 (1982).

[20] N. R. Avery, Chem. Phys. Lett. **96**, 371 (1983).

[21] G. Kresse and J. Hafner, Phys. Rev. B **47**, R558 (1993).

[22] G. Kresse and J. Furthmüller, Phys. Rev. B **54**, 11 169 (1996); Comput. Mater. Sci. **6**, 15 (1996).

[23] D. Vanderbilt, Phys. Rev. B **41**, 7892 (1990); G. Kresse and J. Hafner, J. Phys.: Condens. Matter **6**, 8245 (1996).

[24] J. P. Perdew and A. Zunger, Phys. Rev. B **23**, 5048 (1981).

[25] J. P. Perdew, J. A. Chevary, S. H. Vosko, K. A. Jackson, M. R. Pederson, D. J. Singh, and C. Fiolhais, Phys. Rev. B **46**, 6671 (1992).

[26] A. Eichler, F. Mittendorfer, and J. Hafner (unpublished).

[27] A. Eichler and J. Hafner, J. Chem. Phys. **109**, 5585 (1998).

[28] A. Eichler and J. Hafner, Phys. Rev. B **57**, 10 110 (1998).

[29] M. Methfessel and A. Paxton, Phys. Rev. B **40**, 3616 (1989).

[30] G. Mills, H. Jónsson, and G. K. Schenter, Surf. Sci. **324**, 305 (1995).

[31] K. L. Kostov, P. Jakob, and D. Menzel, Surf. Sci. **377-379**, 802 (1997).

[32] C. Stampfl and M. Scheffler, Surf. Sci. **377-379**, 808 (1997); Phys. Rev. Lett. **78**, 1500 (1997); J. Vac. Sci. Technol. A **15**, 1635 (1997).

[33] A. Alavi, P. Hu, Th. Deutsch, P. L. Silvestrelli, and J. Hutter, Phys. Rev. Lett. **80**, 3650 (1998).

[34] J. Wintterlin, S. Völkening, T. V. W. Janssens, T. Zambelli, and G. Ertl, Science **278**, 1931 (1997).

[35] J. L. Gland, B. A. Sexton, and G. B. Fisher, Surf. Sci. **95**, 587 (1980).